First-principles study of γ-CuI for p-type transparent conducting materials

Dan Huang[1]**, Yu-Jun Zhao**[2]**, Shen Li**[3]**, Chang-Sheng Li**[1]**, Jian-Jun Nie**[1]**, Xin-Hua Cai**[1] **and Chun-Mei Yao**[1]

[1] Department of Physics and Electronic Sciences, Hunan University of Arts and Science, Changde 415000, People's Republic of China
[2] Department of Physics and State Key Laboratory of Luminescent Materials and Devices, South China University of Technology, Guangzhou 510640, People's Republic of China
[3] State Key Lab of Superhard Materials, Jilin University, Changchun 130012, People's Republic of China

E-mail: danhuangdan@gmail.com

Abstract

γ-CuI has attracted considerable attention recently as a p-type transparent conductive material. In this paper, we have investigated the hole effective mass, intrinsic defects and group VI-A impurities in γ-CuI by first-principles calculations. We found that the hole effective mass of γ-CuI is light, in line with the high p-type mobility observed in experiments. The p-type conductance is expected to originate from Cu vacancies, which have a low formation energy with no significant n-type compensating defects. The relative high transition level of Cu vacancy, however, may lead to a low hole concentration in the γ-CuI sample. Additionally, no shallow transition levels were found in γ-CuI with substitutional group VI-A impurities at I sites.

(Some figures may appear in colour only in the online journal)

1. Introduction

Transparent conducting materials (TCMs) constitute a class of materials in which carrier conductivity coexists with optical transparency, a combination useful for optoelectronic applications [1]. The most popular TCMs are n-type Sn-doped In_2O_3 (ITO) [2], F-doped SnO_2 (FTO) [3] and Al-doped ZnO (AZO) [4], which are used for front surface electrodes of solar cells and flat panel displays, low-emissivity windows, touch-panel control, defrosting windows of aircraft, static dissipation layer and so on. Unfortunately, their advanced functions based on p–n junction have not been practically realized, since suitable p-type TCMs are rare as most of the existing TCMs are n-type. Therefore, it is crucial to find an excellent p-type TCM for a possible transparent electronic era [5].

In 1997, Kawazoe *et al* [6] first reported p-type conductivity in $CuAlO_2$ with delafossite structure, which has room temperature p-type conductivity up to $1\,S\,cm^{-1}$. Following that study, other delafossite-type materials, such as $CuBO_2$ [7], $CuScO_2$ [8] and $CuCrO_2$ [9], have been shown to possess p-type conductivity. Nie *et al* [10] revealed from first-principles studies that this delafossite family does not exhibit a

direct band gap. This may impede the application of delafossite $CuM^{III}O_2$ since TCMs with a direct band gap are preferred for the p–n junctions [11].

In addition to the delafossite family, γ-CuI and chalcopyrite $CuAlS_2$ with zinc-blende structure and direct band gap have also been reported to display p-type conductivity. The zinc-blende structure is easy to match with other conventional semiconductors and the direct band gap is also beneficial for the preparation of p–n junctions, which push γ-CuI and $CuAlS_2$ [12, 13] as promising p-type TCM candidates. Here, we place our focus on γ-CuI. Sirimanne *et al* [14, 15] prepared polycrystalline γ-CuI films by three different techniques. The films with the best property showed an optical transmittance of over 80% in the wavelength range 400–900 nm and a minimum resistivity of about $60\,\Omega\,cm$. Based on the pulsed laser deposition technique, Zhu *et al* [16] prepared CuI films which showed resistivity in the order of $10^{-1}\,\Omega\,cm$ and optical transmittance over 80% in the wavelength range 410–1000 nm. Recently, Chen *et al* [17] obtained a large-sized high-quality single crystal γ-CuI by the hydrothermal method. The crystal showed a high p-type

mobility of 43.9 cm^2 V^{-1} S^{-1}, with a low hole concentration of 4.3×10^{16} cm^{-3}, which largely fails the criterion for applications ($>10^{20}$ cm^{-3}). They also speculated that the p-type conductivity arises from Cu vacancies.

In this paper, we have investigated the intrinsic/extrinsic defects and hole effective mass in γ-CuI with DFT-GGA and DFT-GGA+U. Our results showed that the hole effective mass is light, consistent with the reported high p-type mobility. We also found that GGA + U provides a more reasonable defect formation energy for the intrinsic and extrinsic defects in γ-CuI, and the p-type conductance is attributed to the Cu vacancies. To seek other possible shallow p-type defects, we have investigated the defects of group VI-A elements doped at I sites in γ-CuI. Unfortunately, it is found that the defect levels of these defects are not shallow in γ-CuI.

2. Computational details

Our first-principles calculations were carried out with the density functional theory (DFT) as implemented in the Vienna Ab-initio Simulation Package (VASP) [18, 19]. The exchange and correlation functional is chosen as a GGA-PBE formalism [20]. It is well known that GGA performance for defects in Cu-oxides is very poor [21, 22], hence special care is taken for CuI. Here, we performed both GGA and GGA + U [23] calculations for a comparison. The value of U_{eff} employed for the Cu d states is 5.2 eV, in line with the values adopted in previous studies [24, 25]. To describe the interactions between the valence electrons (Cu:3d^{10}4s^1, I:5s^{2}5p^5) and the core, the projector augmented wave (PAW) implementation [26] was used. For the γ-CuI unit cell, a special K-point sampling over a $6 \times 6 \times 6$ Monkhorst–Pack mesh [27] is used, including the HSE06 [28] calculation of the band gap. For all the calculations, the energy cutoff of 500 eV is used. For the formation energy calculation, $2 \times 2 \times 2$ supercells containing 64 atoms are used. A $3 \times 3 \times 3$ K-point mesh is employed for the $2 \times 2 \times 2$ supercells. Furthermore, a $3 \times 3 \times 3$ supercell with a K mesh of $2 \times 2 \times 2$ is used for the convergence test of formation energy by GGA + U, showing that the change in the formation energy and transition level is less than 0.01 eV.

CuI has three kinds of crystal structures, including a zinc-blende-type structure (γ-phase) [29] at low temperatures, a fluorite-type structure (α-phase) [30] at high temperatures, and an intermediate β-phase of hexagonal structure [31] between the γ- and α-phases. Our calculated lattice parameters of γ-CuI are $a = b = c = 6.088$ Å, 6.115 Å and 6.102 Å from GGA, GGA + U and HSE06, respectively, in good agreement with the experimental value of 6.1 Å [29]. For the doped supercells, the lattice constants are fixed at its GGA or GGA + U calculated crystal length, respectively, and the internal coordinates are fully relaxed.

3. Results and discussion

Figure 1 shows the partial density of state (PDOS) and band structure of γ-CuI from GGA and GGA + U calculations. The characteristics of the band structures are similar for the GGA and GGA + U results. The majority of the lower valence

bands (around -6 to -4 eV with respect to the Fermi level) are dominated by Cu 3d and I 5p, and the majority of the upper valence bands (around -2.5 to -0 eV) are dominated by Cu 3d with a noticeable contribution from I 5p. Here, we could see that the width of the upper valence bands increases from 2.0 eV by GGA to 2.6 eV after +U correction according to the band structure in figure 1. The lower conduction band consists of Cu 4s, I 6s and I 5p. The splitting between the lower valence bands and the upper valence bands are different from GGA and GGA + U. Since the valence band mainly comes from Cu 3d, it becomes more localized and has a larger band gap when the on-site Hubbard U is applied to the Cu 3d orbital. Both the GGA and GGA + U results showed that γ-CuI is a direct band gap semiconductor with the valence band maximum (VBM) and conduction band minimum (CBM) at Γ point in the Brillouin zone. Our calculated GGA, GGA+U and HSE06 band gaps are 1.12 eV, 1.89 eV and 2.56 eV respectively. All of them are smaller than the experimental value, 3.1 eV [32, 33]. The energy band at the VBM is threefold degenerated. This disappears along Γ–K and evolves to a twofold degenerated state and a single state along Γ–X and Γ–L. In order to obtain the carrier effective masses, we calculated the energy eigenvalue at a definite K-point along special axes from DFT. Then, we fit the actual E–K diagram around CBM or VBM with a parabola. According to the following equation:

$$\frac{1}{m^*(k)} = \frac{1}{\hbar} \frac{\partial^2 E(k)}{\partial k^2}, \tag{1}$$

we got the carrier effective masses $m^*(k)$. The GGA and GGA+U calculated carrier effective masses of γ-CuI are listed in table 1. The carrier effective mass values from GGA and GGA + U are similar to each other along all the studied axes in the reciprocal space. The value of effective mass of the light holes (0.2–$0.25 m_e$) has the same order as that of the good n-type TCM In$_2$O$_3$, in which the electron effective mass is $0.24 m_e$ [34]. This is clearly consistent with the experimental observation of high p-type mobility in γ-CuI [17].

In addition to the hole mobility μ_p ($\mu_p = q\tau_p/m^*$), the p-type conductance σ ($\sigma = pq\mu_p$) relies on the hole concentration p, which depends on the doping concentration and the transition level of defects at a given temperature. The doping concentration is in fact determined by the defect formation energy, which depends on the sample preparation condition through the equilibrium of related chemical potentials. The transition level of a defect $\varepsilon(D, q/q')$ can also be deduced from the defect formation energy as

$$\varepsilon(D, q/q') = \frac{\Delta E(D, q) - \Delta E(D, q')}{q' - q}. \tag{2}$$

The formation energies for the intrinsic and extrinsic defects are calculated with a $2 \times 2 \times 2$ γ-CuI supercell according to [35]:

$$\Delta E(D, q) = E(D, q) - E(0) + \sum_\alpha n_\alpha (\Delta\mu_\alpha + \mu_\alpha^{solid})$$
$$+ q(E_{VBM} + E_F), \tag{3}$$

where $E(D, q)$ and $E(0)$ are the total energies of the supercells with and without defects. Here $(\Delta\mu_\alpha + \mu_\alpha^{solid})$ is the absolute
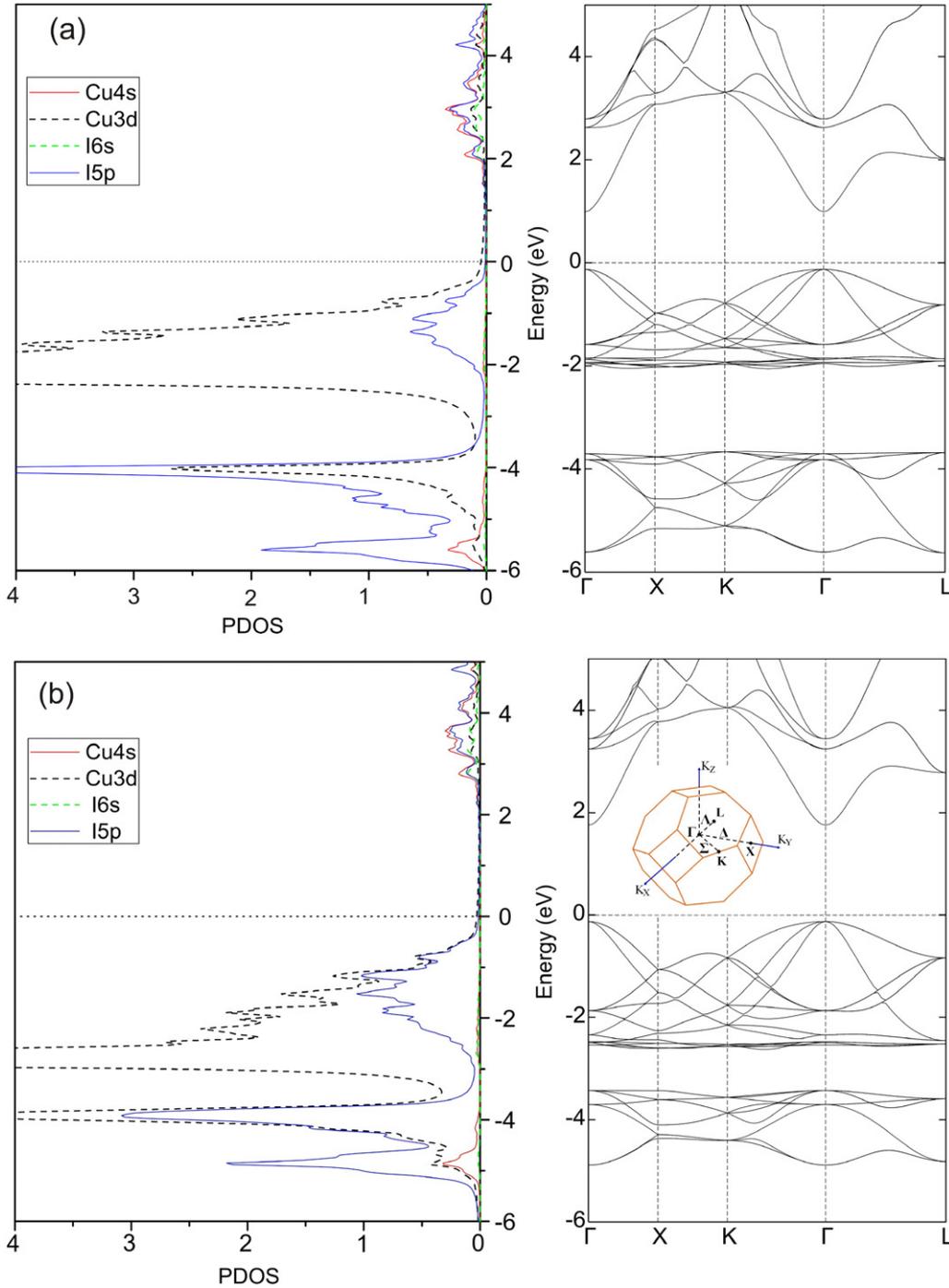
Figure 1. PDOS and band structure of γ-CuI from GGA (*a*) and GGA + U (*b*), and the Brillouin zone of γ-CuI is inserted in the band gap plot from GGA + U.

value of the chemical potential of atom α. $\mu_\alpha^{\mathrm{solid}}$ is defined as the chemical potential of the elemental solid. Also n_α is the number of atoms related to the defect; $n_\alpha = -1$ if an atom is added, while $n_\alpha = 1$ if an atom is removed. E_{VBM} represents the energy of the VBM of the defect-free system and E_{F} is the Fermi energy relative to the E_{VBM}. For charged systems, a compensating homogeneous jellium background charge is assumed to preserve overall neutrality. Recently, Lany and Zunger [36] found that the formation energy of GaAs : V_{As}^{3+} could be well converged in fairly small supercells such as a 64-atom or even 32-atom supercell, as long as the

potential alignment and image charge correction are included. Considering the 64-atom supercells adopted in this work, we have carried out the calculations with both potential alignment and image charge correction. The potential alignment is considered by adding ΔV into the $(E_{\mathrm{VBM}} + E_{\mathrm{F}})$ term, where ΔV is the electrostatic alignment between the doped host and the pure host according to the electrostatic potential of I atom in the core region (for the doped system, the I atom is chosen with the furthest one away from the defect in the supercell). Up to the third order, image charge correction is applied in this work by a simple scaling factor (2/3) to the first-order

Table 1. Effective mass of electrons and holes in γ-CuI from GGA and GGA + U calculations (unit: m_e).

		GGA				
Hole	m_{001}	0.24	m_{011}	0.20	m_{111}	0.20
		0.76 (twofold)		0.72		1.61 (twofold)
				3.34		
Electron	m_{001}	0.16	m_{011}	0.17	m_{111}	0.18
		GGA + U				
Hole	m_{001}	0.25	m_{011}	0.21	m_{111}	0.20
		0.75 (twofold)		0.75		1.55 (twofold)
				3.26		
Electron	m_{001}	0.19	m_{011}	0.20	m_{111}	0.20

(screened) Madelung term, as suggested by Lany and Zunger [36]. Here, as a convergence test, we used a $3 \times 3 \times 3$ supercell containing 216 atoms to calculate the formation energy and transition level of Cu vacancy by GGA + U. We found that the change in the formation energy and transition level is less than 0.01 eV.

Our calculated enthalpy of γ-CuI is -0.320 eV and -0.648 eV from GGA and GGA + U, respectively. The GGA + U calculated formation enthalpy is in good agreement with the experimental value of -0.703 eV [37], while the GGA value deviates by $\sim$50%. Figure 2 shows the formation energy of the intrinsic defects in γ-CuI under Cu-poor and Cu-rich conditions from GGA and GGA + U calculations. The formation energy and transition level of various defects under Cu-rich condition are also listed in table 2. The Cu-rich condition corresponds to $\Delta\mu_{Cu} = 0$ and $\Delta\mu_I = \Delta H(CuI)$, while the Cu-poor condition is set to $\Delta\mu_I = 0$ and $\Delta\mu_{Cu} = \Delta H(CuI)$. Here, $\Delta H(CuI)$ is the calculated formation enthalpy of CuI. The calculated (-/0) transition levels of Cu vacancy are 0.18 eV and 0.21 eV from the GGA and GGA+U, respectively. Other p-type defects such as interstitial I (I_{int}) and I substituting Cu (I_{Cu}) have substantially higher formation energy than the Cu vacancy, and thus they are not expected to contribute to the p-type conductance effectively. Since Cu vacancy has the lowest formation energy even under Cu-rich conditions from both GGA and GGA + U results, it is confirmed that the p-type conductance originates from the Cu vacancy (V_{Cu}). The other n-type defects such as interstitial Cu (Cu_{int}) and I vacancy (V_I) also have a higher formation energy than Cu vacancy. So there is no remarkable n-type compensating defect to impede the hole carriers.

It is noted that the formation energy of Cu vacancy from GGA is always less than zero under both Cu-rich and Cu-poor conditions. This could be unphysical since the negative formation energy implies that Cu vacancies would be spontaneously formed even under Cu-rich conditions, unless a large repulsion exists between the Cu vacancies to avoid the evolution of defects. Meanwhile, it is known that LDA or GGA generally has a considerable error on the heat of formation of the compounds. Although the errors could be cancelled out to a certain degree for chemically similar systems, it may bring about quite large errors for chemically unalike systems and result in a negative defect formation energy within the calculated stable boundary of the host compound [38]. It could be attributed to the inconsistent description of GGA on Cu 3d orbitals in CuI and bulk Cu.

GGA+U calculated formation energy of Cu vacancy is positive under Cu-rich conditions. Under Cu-poor conditions, the GGA + U calculated formation energy of Cu vacancy is also slightly below zero near VBM. Nagoya *et al* [39] found that the formation energy of Cu vacancy would increase with increasing concentration of Cu vacancy in another p-type semiconductor Cu_2ZnSnS_4. This indicates that the Cu vacancy in γ-CuI can also be thermodynamically stable up to a fairly high concentration under Cu-poor conditions. Therefore, we conclude that GGA + U provides a more reasonable result on defect formation energy in γ-CuI than that based on GGA calculation, though the transition levels of Cu vacancy do not change remarkably. If there are 5% unoccupied Cu sites in γ-CuI, the calculated hole concentrations are 8.7×10^{16} cm^{-3} and 2.7×10^{16} cm^{-3} under room temperature corresponding to the thermal ionization energies from GGA (0.18 eV) and GGA + U (0.21 eV), respectively. Therefore, the low hole concentration ($\sim 4.3 \times 10^{16}$ cm^{-3}) of γ-CuI from experiment could be attributed to the relatively deep defect transition level of Cu vacancy, other than the possible n-type compensating defects, or high formation energy of p-type defects.

Since the hole concentration in γ-CuI needs to be improved for practical applications, we attempted to search for other possible shallow dopants in γ-CuI. Group VI-A elements (O, S, Se and Te) are expected to be p-type dopants when doped on I sites, though no related experiments have been reported to the best of our knowledge. We calculated the formation energies and transition levels of group VI-A elements doped on I sites. Figure 3 shows the formation energies of the substitutional defects of group VI-A elements on I sites in γ-CuI under Cu-rich conditions from both GGA and GGA + U with regard to the Fermi level. In order to avoid precipitation of impurity phases, the chemical potentials of group VI-A elements are limited by the formation enthalpies of Cu_2O, Cu_2S, Cu_2Se, CuTe, etc under Cu-rich conditions. Unfortunately, we did not find any shallow levels from the substitutional group VI-A defects in γ-CuI. The calculated (-/0) transition levels for O_I, S_I, Se_I and Te_I are 0.28, 0.29, 0.31 and 0.36 by GGA and 0.29, 0.33, 0.37 and 0.45 by GGA + U, respectively, in line with the sequence of their electronegativities. But the formation energies of the substitutional defects show some discrepancy from GGA and GGA + U calculations. The formation energies of S and Se doping are positive from GGA + U but negative from GGA. Combined with the former results on intrinsic defects, such as Cu vacancy, we found that the GGA and GGA + U results do
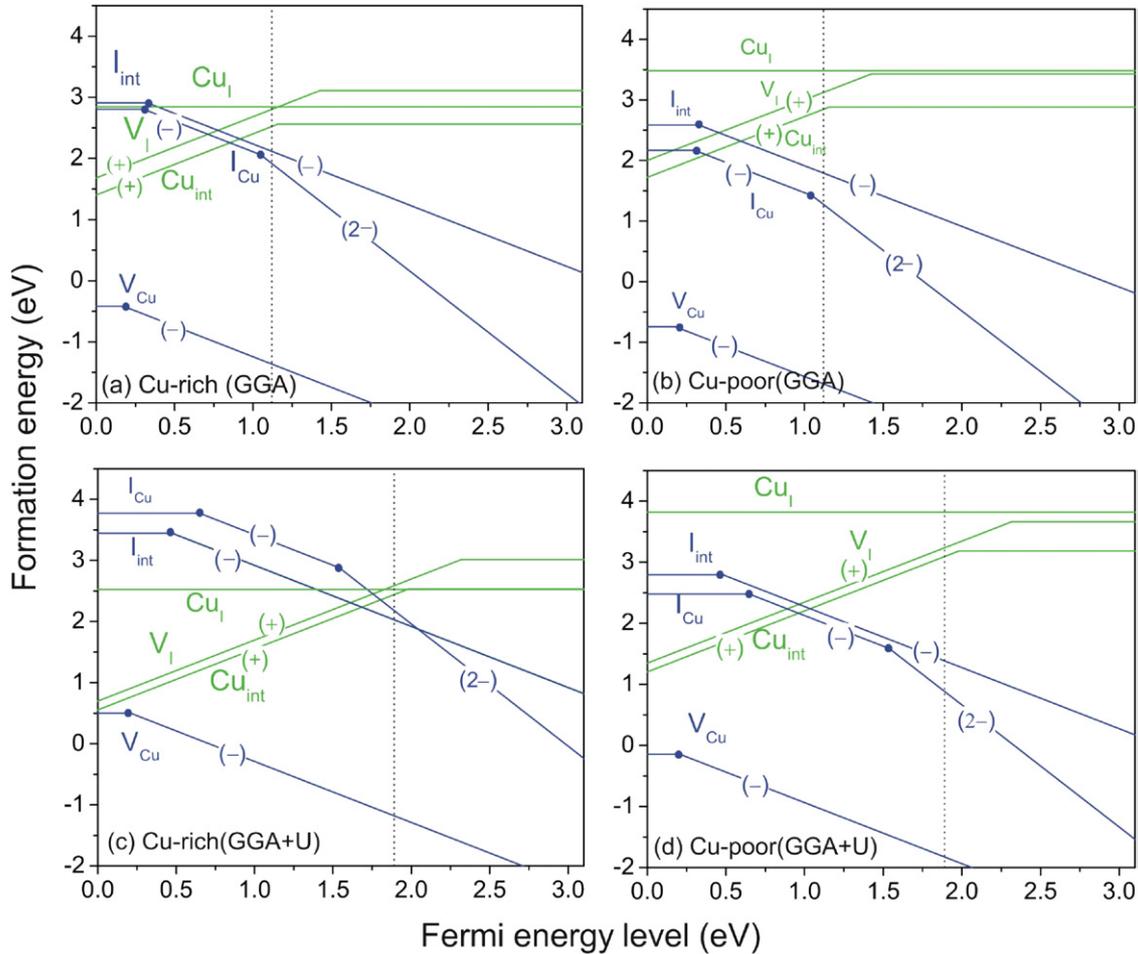
Figure 2. Formation energy of intrinsic defects in γ-CuI under various conditions from GGA (*a*), (*b*) and GGA + U (*c*), (*d*). Blue and green lines represent the acceptor and donor defects, respectively. Here the experimental gap of γ-CuI $E_g = 3.1$ eV is adopted, with the vertical dashed line reflecting the calculated band gap.

not show large difference on the transition level of defects, but some discrepancy on defect formation energy.

In addition, the calculated bond lengths are 1.96 Å, 2.22 Å, 2.36 Å and 2.51 Å from GGA and 1.96 Å, 2.23 Å, 2.36 Å and 2.52 Å from GGA + U for Cu–O_I, Cu–S_I, Cu–Se_I and Cu–Te_I in their neutral defect charge state, respectively. The GGA and GGA + U calculated bond lengths have little deviation from each other, as the bond length of Cu–I in pure γ-CuI; 2.64 Å from GGA and 2.65 Å from GGA + U. Recently, Mao *et al* [40] found that there was a large mobility enhancement (10^3–10^4 times) by In–Ga co-doping in SnO_2 compared with the single doping of In or Ga. Owing to the ions radius following the sequence $Ga^{3+} < Sn^{4+} < In^{3+}$, In–Ga co-doping can effectively decrease SnO_2 lattice distortion compared with In-doped and Ga-doped SnO_2. This shows that the lattice distortion has an important effect on mobility. Group VI-A elements doped at I sites are expected to induce lattice distortion and thus a lower hole mobility. Therefore, we expect that group VI-A elements may not be good p-type dopants for γ-CuI to improve its p-type conductivity. To decrease the transition level, co-doping of n- and p-type dopants to produce an impurity band above the VBM may be a possible approach [41, 42].

4. Conclusion

In summary, we have calculated the hole effective mass, intrinsic defects and group VI-A impurities in γ-CuI by GGA and GGA + U calculations. The effective masses of light holes are around 0.2–0.25 m_0, consistent with the high p-type mobility from experiments. Through the formation energy of various intrinsic defects, we demonstrated that the p-type conductance is ascribed to the Cu vacancies. The low hole concentration could be explained by the relatively deep transition level of Cu vacancies. The calculated transition levels of group VI-A impurities at I sites are not shallow either. To obtain shallow transition levels and thus a high hole concentration in γ-CuI, new approaches are suggested, such as co-doping of n- and p-type impurities.

Acknowledgments

Table 2. Defect formation energies $\Delta E(D, q)$ and defect transition levels $\varepsilon(D, q/q')$ in CuI under Cu-rich conditions (E_V and E_C represent the calculated VBM and CBM, respectively).

|	GGA	GGA + U
Defect	$\Delta E(D, q)$ (eV)	$\Delta E(D, q)$ (eV)
V_{Cu}^0	-0.43	0.5
V_{Cu}^-	-0.25	0.71
	$\varepsilon: (-/0) = E_V + 0.18$ eV	$\varepsilon: (-/0) = E_V + 0.21$ eV
I_{Cu}^0	2.80	3.77
I_{Cu}^-	3.10	4.42
I_{Cu}^{2-}	4.15	5.96
	$\varepsilon: (-/0) = E_V + 0.30$ eV	$\varepsilon: (-/0) = E_V + 0.65$ eV
	$\varepsilon: (2-/-) = E_V + 1.05$ eV	$\varepsilon: (2-/-) = E_V + 1.54$ eV
I_{int}^0	2.91	3.45
I_{int}^-	3.24	3.93
	$\varepsilon: (-/0) = E_V + 0.33$ eV	$\varepsilon: (-/0) = E_V + 0.48$ eV
Cu_{int}^+	1.40	0.55
Cu_{int}^0	2.56	2.54
	$\varepsilon: (0/+) = E_C + 0.04$ eV	$\varepsilon: (0/+) = E_C + 0.09$ eV
V_I^+	1.68	0.70
V_I^0	3.11	3.02
	$\varepsilon: (0/+) = E_C + 0.31$ eV	$\varepsilon: (0/+) = E_C + 0.43$ eV
Cu_I^0	2.84	2.53
O_I^0	1.10	1.71
O_I^-	1.38	2.00
	$\varepsilon: (-/0) = E_V + 0.28$ eV	$\varepsilon: (-/0) = E_V + 0.29$ eV
S_I^0	-0.05	0.70
S_I^-	0.24	1.03
	$\varepsilon: (-/0) = E_V + 0.29$ eV	$\varepsilon: (-/0) = E_V + 0.33$ eV
Se_I^0	-0.18	0.72
Se_I^-	0.13	1.09
	$\varepsilon: (-/0) = E_V + 0.31$ eV	$\varepsilon: (-/0) = E_V + 0.37$ eV
Te_I^0	0.22	0.63
Te_I^-	0.58	1.08
	$\varepsilon: (-/0) = E_V + 0.36$ eV	$\varepsilon: (-/0) = E_V + 0.45$ eV
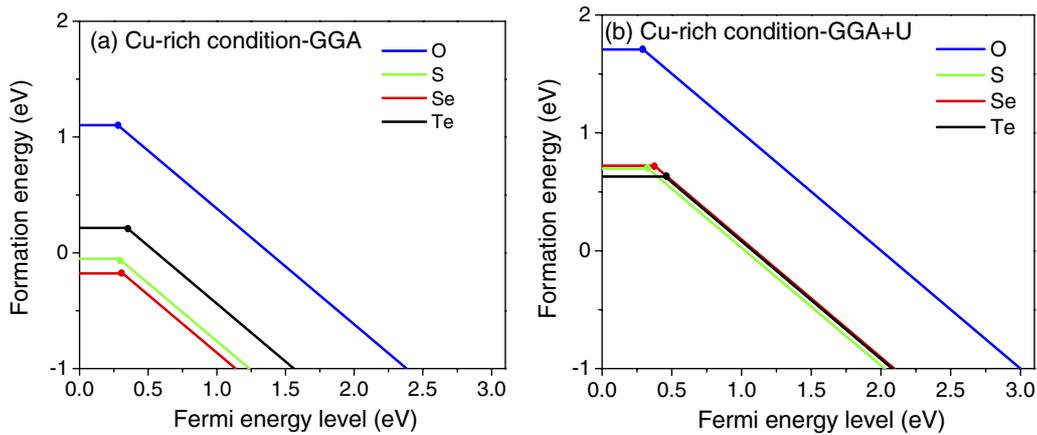
Figure 3. Formation energy of group VI-A elements doped on I sites in γ-CuI under Cu-rich conditions both from GGA (*a*) and GGA + U (*b*). Here the experimental gap of γ-CuI $E_g = 3.1$ eV is adopted.

References

[1] Gordon R G 2000 *MRS Bull.* **25** 52
[2] Harvey S P *et al* 2006 *J. Phys. D: Appl. Phys.* **39** 3959
[3] Remes Z *et al* 2009 *Thin Solid Films* **517** 6287
[4] Wu K Y *et al* 2007 *Nanotechnology* **18** 305604
[5] Thomas G 1997 *Nature* **389** 907
[6] Kawazoe H *et al* 1997 *Nature* **389** 939
[7] Snure M and Tiwari A 2007 *Appl. Phys. Lett.* **91** 092123
[8] Duan N *et al* 2000 *Appl. Phys. Lett.* **77** 1325
[9] Nagarajan R *et al* 2001 *J. Appl. Phys.* **89** 8022
[10] Nie X L *et al* 2002 *Phys. Rev. Lett.* **88** 066405
[11] Godinho K G *et al* 2010 *J. Mater. Chem.* **20** 1086

J. Phys. D: Appl. Phys. **45** (2012) 145102

D Huang *et al*

[12] Huang D *et al* 2010 *J. Phys. D: Appl. Phys.* **43** 395405
[13] Huang D *et al* 2011 *J. Appl. Phys.* **109** 113714
[14] Sirimanne P M *et al* 2003 *Mater. Chem. Phys.* **80** 461
[15] Sirimanne P M *et al* 2002 *Chem. Phys. Lett.* **366** 485
[16] Zhu B L and Zhao X Z 2011 *Phys. Status Solidi* a **208** 91
[17] Chen D G *et al* 2010 *Cryst. Growth Des.* **10** 2057
[18] Kresse G and Hafner J 1993 *Phys. Rev.* B **47** 558
[19] Kresse G and Furthmüller J 1996 *Phys. Rev.* B **54** 11169
[20] Perdew J P *et al* 1996 *Phys. Rev. Lett.* **77** 3865
[21] Scanlon D O *et al* 2009 *Phys. Rev. Lett.* **103** 096405
[22] Scanlon D O *et al* 2009 *J. Chem. Phys.* **131** 124703
[23] Dudarev S L *et al* 1998 *Phys. Rev.* B **57** 1505
[24] Scanlon D O *et al* 2010 *J. Chem. Phys.* **132** 024707
[25] Scanlon D O *et al* 2009 *Phys. Rev.* B **79** 035101
[26] Kresse G and Joubert J 1999 *Phys. Rev.* B **59** 1758
[27] Monkhorst H J and Pack J D 1976 *Phys. Rev.* B **13** 5188
[28] Krukau A V *et al* 2006 *J. Chem. Phys.* **125** 224106
[29] Bhalla A S and White E W 1971 *Acta Crystallogr.* B **27** 852
[30] Yude Y *et al* 1990 *Z. Kristallogr.* **191** 79
[31] Buehrer W and Haelg W 1977 *Electrochim. Acta* **22** 701
[32] Bouhafs B *et al* 1998 *Phys. Lett.* A **240** 257
[33] Sekkal W and Zaoui A 2002 *Physica* B **315** 201
[34] Walsh A *et al* 2008 *Phys. Rev.* B **78** 075211
[35] Zhang S B *et al* 2001 *Phys. Rev.* B **63** 075205
[36] Lany S and Zunger A 2008 *Phys. Rev.* B **78** 235104
[37] Lide D R (ed) 2007 *CRC Handbook of Chemistry and Physics* 88th edn (Boca Raton, FL: CRC Press/Taylor and Francis)
[38] Lany S 2008 *Phys. Rev.* B **78** 245207
[39] Nagoya A *et al* 2010 *Phys. Rev.* B **81** 113202
[40] Mao Q N *et al* 2010 *Phys. Status Solidi* b **247** 299
[41] Yan Y F *et al* 2007 *Phys. Rev. Lett.* **98** 135506
[42] Gai Y Q *et al* 2009 *Phys. Rev.* B **80** 153201